Original

An L314Q mutation in *Map3k1* gene results in failure of eyelid fusion in the N-ethyl-N-nitrosourea-induced mutant line

Bing CHEN[1–3]*, Hong-Ling WANG[2]*, Rui CHEN[2]*, Li CHEN [2], Shun YANG[2], Yi WANG [2] and Zheng-Feng XUE[1–3]

[1)]*Institute of Comparative Medicine, Yangzhou University, 12 Wenhui East Road, Yangzhou, Jiangsu Province 225009, P.R.China*
[2)]*College of Veterinary Medicine, Yangzhou University, 12 Wenhui East Road, Yangzhou, Jiangsu Province 225009, P.R.China*
[3)]*Jiangsu Co-innovation Center for Prevention and Control of Important Animal Infectious Diseases and Zoonoses, Yangzhou University, 12 Wenhui East Road, Yangzhou, Jiangsu Province 225009, P.R.China*

Abstract: In this study, we describe an N-ethyl-N-nitrosourea-induced mouse model with a corneal opacity phenotype that was associated with "eye open at birth" (EOB). Histological and immunohistochemistry staining analysis showed abnormal differentiation of the corneal epithelial cells in the mutant mice. The EOB phenotype was dominantly inherited on a C57BL/6 (B6) background. This allele carries a T941A substitution in exon 4 that leads to an L314Q amino acid change in the open reading frame of MAP3K1 (MEEK1). We named this novel *Map3k1* allele *Map3k1^{L314Q}*. Phalloidin staining of F-actin was reduced in the mutant epithelial leading edge cells, which is indicative of abnormality in epithelial cell migration. Interestingly enough, not only p-c-Jun and p-JNK but also c-Jun levels were decreased in the mutant epithelial leading edge cells. This study identifies a novel mouse *Map3k1* allele causing EOB phenotype and the EOB phenotype in *Map3k1^{L314Q}* mouse may be associated with the reduced level of p-JNK and c-Jun.
Key words: c-Jun, eye open at birth (EOB), *Map3k1*, mouse, N-ethyl-N-nitrosourea (ENU)

Introduction

Mammalian normal ocular surface development involves transient closure and reopening of the eyelid. Eyelid closure has been best characterized in mice. During the embryonic stage, the epithelium of the upper and lower eyelid fuses to form a closed eyelid as a protective barrier over the cornea. About two weeks after birth, the cells present at the fusion junction undergo apoptosis and result in separation of the upper and lower eyelids [1–3]. Failure of the eyelids to grow across the eye and fuse during the foetal stage in mice leads to the "eye open at birth" (EOB) phenotype [4–6].

Transient lid closure and reopening is a common mor-

phogenetic event that also takes place in humans. Unlike the mouse eyelid, however, human eyelid closure and re-opening is accomplished entirely in utero; this makes it difficult to detect deficiencies in human eyelid closure. This has made the detection of lid closure defects a major challenge, and as a result, little is truly understood about the incidence of eyelid closure defects and the diseases associated with it in humans [7–9]. In this context, genetic EOB mouse models with an easily traceable phenotype have made it possible to identify a great number of molecular players involved in eyelid development, including MEK kinase1 (*Map3k1*), c-Jun N-terminal kinase (*Jnk1* and *Jnk2*), *c-Jun*, *Alx4*, *Lgr4*, epidermal growth factor (EGF) family members HB-EGF (*Hbegf*)

and transforming growth factor α*(Tgfa)* and their receptor (*Egfr*), fibroblast growth factor 10 (*Fgf10*) and its receptor (*Fgfr2*), the forkhead transcription factors *Foxc1* and *Foxc2*, and the *Wnt* antagonist *Dkk2* [10–32]. This information may help to identify developmental defects associated with lid closure failure and their underlying mechanisms in humans.

MAP3K1, also known as MEK kinase 1 (MEKK1), is one of the most prominent players that control eyelid morphogenesis, and it is expressed abundantly in the epithelial cells. With the help of an N-ethyl-N-nitrosourea (ENU) mutagenesis screen, we identified a mouse mutant, *Map3k1^{L314Q}*, which carries an L314Q mutation in the *Map3k1* gene. We were able to show a clear decrease in the levels of JNK phosphorylation and c-Jun indicated that the EOB phenotype may be associated with the reduced level of p-JNK and c-Jun.

Materials and Methods

Mice

C57BL/6J male mice were injected intraperitoneally with 100 mg/kg of ENU weekly for three weeks, left for two months and then mated to untreated female C57BL/6J mice. The offspring of the ENU-treated mice were screened at the age of 3 weeks for dysmorphological phenotype.

All animal protocols were approved by the Institutional Animal Care and Use Committee (IACUC) of the Yangzhou University Animal Experiments Ethics Committee, and carried out in accordance with the approved guidelines.

Preparation of DNA and RNA

Genomic DNA was isolated from mouse tail tips by proteinase K digestion, phenol chloroform extraction, and ethanol precipitation according to standard protocols. Total RNA was extracted from the brains of *Map-3k1^{L314Q}* heterozygotes (*Map3k1^{L314Q/+}*) and wild-type mice using TRIzol reagent (Invitrogen, Carlsbad, CA, USA) according to the manufacturer's instructions.

Linkage analysis

Map3k1^{L314Q/+} of the B6 background were mated with DBA/2 (D2) mice to generate F1 mice. Next, F1 mice with EOB were backcrossed with B6 mice to generate N2 mice. DNA samples of the N2 mutant mice were scanned using microsatellite and single nucleotide polymorphism (SNP) markers.

Mutational analysis of *Map3k1*

The exons sequences of *Map3k1* were amplified from *Map3k1^{L314Q/+}* and B6 cDNA and genomic DNA using PCR. cDNA was synthesized using a RevertAid First-Strand cDNA Synthesis Kit (Thermo Scientific Fermentas, St. Leon-Ro,Germany) with oligo(dT)18 primers. PCR conditions consisted of one cycle of denaturation for 5 min at 94°C, followed by 30 cycles of 30 s at 94°C, 30 s at 61°C, and 1 min at 72°C, and finally, one cycle of elongation for 5 min at 72°C. The RefSeq ID of *Map3k1* is NM_011945. Primer sequences are provided in supplementary Table. RT-PCR and PCR products were purified and sequenced by the dideoxy chain termination method using an ABI310 automated DNA sequencer (Sangon Biotech, Shanghai, China).

Histological analysis

Tissues were fixed in Davidson's fixative or 4% paraformaldehyde at 4°C overnight. The fixed specimens were decalcified, dehydrated and embedded in paraffin wax, and 6-μm sagittal sections were obtained and HE-stained using standard protocols.

Immunohistochemistry

Antigen retrieval with citrate buffer was performed prior to incubation with the antibodies. The following antibodies were used: anti-keratin10 (1:4,000; ABCAM, Cambridge, MA, USA, Cat. ab76318), anti-keratin14 (1:4,000; ABCAM, Cat. ab181595), anti-PAX6 (1:400; Covance, Princeton, NJ, USA, Cat. PRB-278P), anti-keratin12 (1:400; ABCAM, Cat. ab185627), anti-keratin6A (1:400; Covance, Cat. PRB-169P), anti-c-Jun (1:200; Cell Signalling, Danvers, MA, USA, Cat. 9165), anti-phospho-c-Jun (1:80; Cell Signalling, Cat. 2361), and anti-phospho-JNK (1:60; ABCAM, Cat. ab124956). Immune complexes were detected with a biotinylated secondary antibody (1:400; Vector Labs, Burlingame, CA, USA, Cat. BA1000) and ABC complex (Vector Labs, Cat. PK6100), and the DAB substrate kit (Vector Labs, Cat. SK4100), followed by brief counterstaining with Mayer's haematoxylin.

F-actin staining analysis

For F-actin staining analysis, embryo heads (E15.5) were fixed in 4% paraformaldehyde at 4°C for 3 h, and then immersed in 30% sucrose in phosphate-buffered saline (PBS) overnight at 4°C. The tissues were embedded in optimal cutting temperature compound (OCT) and rapidly frozen. Sections of 9-μm thickness were placed on poly-L-lysine-coated slides and fixed in cold acetone. The sections were washed in PBS and incubated in PBS blocking/permeabilization buffer (PBS containing 1% bovine serum albumin, 0.3% Triton X-100 and 1% goat serum) for 15 min. The sections were

then stained with Alexa Fluor® 488-phalloidin (Molecular Probes, Eugene, OR, USA, Cat. A12379) according to the manufacturer's instructions. For staining of nuclei and stabilization of fluorescence signals, the samples were covered with Fluoroshield mounting medium containing DAPI (Sigma, St. Louis, MO, USA, Cat. F6057). The stained sections were photographed with a laser scanning confocal microscope (TCS SP8 STED, Leica, Wetzlar, Germany).

Results

Identification and generation of mutant mice with an EOB phenotype

The founder of the $Map3k1^{L314Q}$ heterozygous mutants ($Map3k1^{L314Q/+}$) was identified from a dominant ENU mutagenesis phenotype-driven screen using C57BL/6 (B6) background mice. The mutant was identified based on its corneal opacity phenotype and dominantly inherited on the B6 background (Fig. 1B). The mutant mouse was mated with wild-type B6 mice to generate mutant offspring.

Histologic examination of the altered corneas in $Map3k1^{L314Q/+}$ mice revealed that the epithelium was markedly thickened and contained an eosinophilic stratum corneum, which was suggestive of the conversion of non-keratinized corneal epithelial cell (CECs) into a keratinized skin-like epithelium. Additionally, corneal neovascularization was detected in the corneal stroma in $Map3k1^{L314Q/+}$ mice (Fig. 1D).

Upon closer examination of the neonates, we observed that the $Map3k1^{L314Q/+}$ pups were uniformly characterized by the EOB phenotype (Figs. 1F and H). On examination of embryos between E16.5 and birth, we found that eyelids from the $Map3k1^{L314Q/+}$ embryos with EOB did not close; this indicates that the phenotype resulted from failure of eyelid closure, and not from premature eyelid opening.

The proportion of mice with the EOB phenotype on a B6 background was 189/382. $Map3k1^{L314Q/+}$ of the B6 background were mated with DBA/2 (D2) mice to generate F1 mice, 12/32 of the progeny were recorded to have the EOB phenotype. When F1 mice with EOB were backcrossed with B6 mice to generate N2 mice, 63/195 the progeny was recorded to have the EOB phenotype. This confirms that the phenotype is dominantly inherited on these backgrounds. However, when the $Map3k1^{L314Q/+}$ mutants with the B6 background were crossed to the 129 background, none of the (B6 × 129) F1 offspring (0/97) exhibited the EOB phenotype. These data show that the EOB phenotype was significantly modified on the 129 background.

Altered corneal epithelial cell differentiation in adult $Map3k1^{L314Q/+}$ mice

The histological findings indicated the pathological conversion of CECs into keratinized skin-like epithelial cells; this implies switches in keratin expression [33]. We, therefore, performed staining for the corneal epithelial cell differentiation marker keratin 12 (K12), the epithelial cell differentiation marker keratin 14 (K14), and a specific epidermal differentiation marker, keratin 10 (K10), by immunohistochemistry in $Map3k1^{L314Q/+}$ and control littermate mice at 8 weeks. Immunohistochemistry showed that K12 was present in the corneal epithelium in the control corneas, but it was absent in the mutant corneas (Figs. 2A and B). In mutant corneas, K10 was expressed most prominently in the suprabasal epithelial layer, and K14 was expressed most prominently in the basal and suprabasal layer of the corneal epithelium (Figs. 2D and F). However, K10 expression was not detected and K14 expression was weak in the wild-type corneal epithelium (Figs. 2C and E). This finding indicates an altered differentiation in adult $Map3k1^{L314Q/+}$ corneas from a cornea-like into a skin-like phenotype.

The transcription factor PAX6 is known to be essential for K12 expression and corneal development [33], and therefore, immunohistochemical staining for PAX6 was also performed. In wild-type mice, PAX6 was expressed in the corneal epithelium (Fig. 2G). In contrast, PAX6 expression was almost abolished in the $Map3k1^{L314Q/+}$ cornea or reduced to low levels in a few cells (Fig. 2H). Thus, loss of PAX6 expression could result in the absence of K12 expression and account for the abnormal differentiation of the corneal epithelium in the adult $Map3k1^{L314Q/+}$ mice.

Mutation analysis of the EOB phenotype

Genomic DNA from 139 N2 EOB mutants was analysed using microsatellite and SNP markers across the whole genome. The mutation was mapped to a 2.16-Mb region on chromosome 13, between microsatellite $D13Mit291$ and SNP $rs3697199$ (Fig. 3A). Within the interval, there was a strong candidate-$Map3k1$. Mice deficient for this gene have previously been shown to exhibit EOB [30, 32].

Sequence analysis identified a T941A substitution in exon 4 that leads to an L314Q amino acid change in the $Map3k1$ (Fig. 3B). Sequence analysis of three different wild-type strains (C3H/He, 129 and DBA/2) excluded the presence of a general polymorphism at this site. Sequence alignment across multiple species revealed that this Lys acid residue is a highly evolutionarily conserved amino acid in $Map3k1$ (data not shown). Thus, the
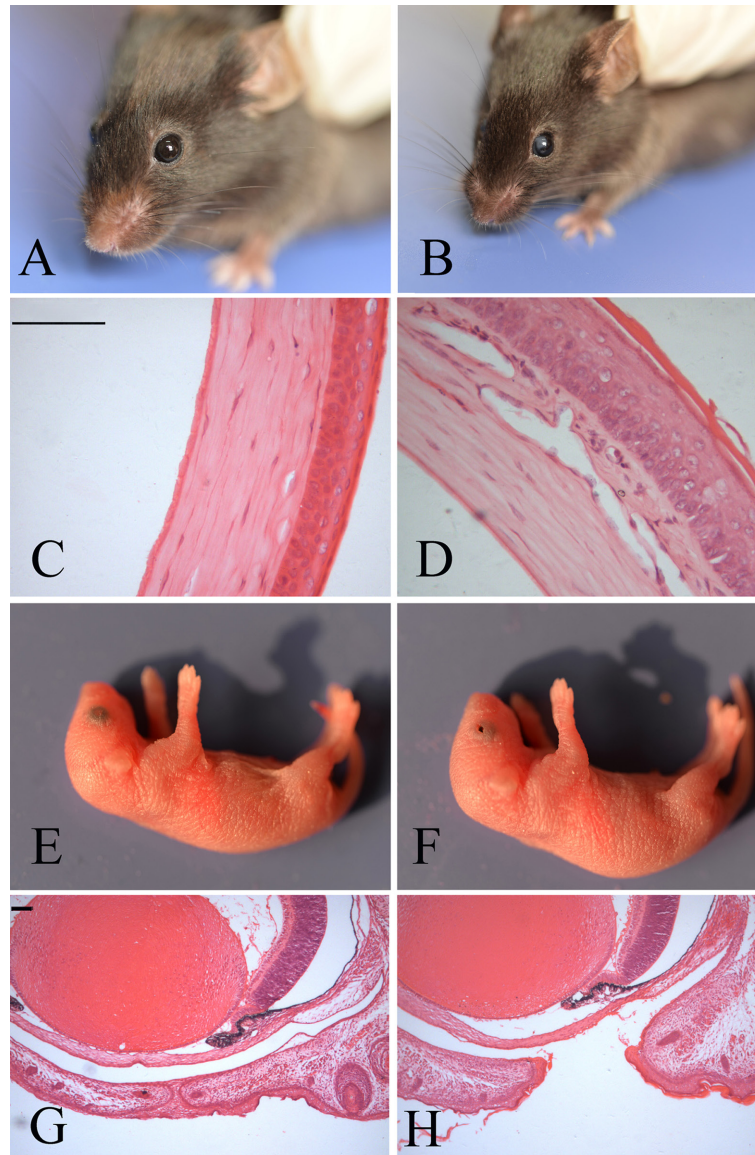
Fig. 1. Eye phenotypes in *Map3k1^{L314Q/+}* mice. (A and B) Appearance of the wild-type (A) and *Map3k1^{L314Q/+}* (B) eyes at week 8. Corneal opacity was observed in the *Map3k1^{L314Q/+}* mice. (C, D) Hematoxylin and eosin staining of frontal eye sections from wild-type (C) and *Map3k1^{L314Q/+}* (D) mice. In *Map3k1^{L314Q/+}* mice, the epithelium was markedly thickened and contained an eosinophilic stratum corneum. (E, F) Appearance of the eyes in wild-type (E) and *Map3k1^{L314Q/+}* (F) mice. *Map3k1^{L314Q/+}* mice are born with open eyelids. (G, H) HE staining of the coronal eye sections from wild-type (G) and *Map3k1^{L314Q/+}* (H) mice at postnatal day 0 (P0). Scale bar=100 μm.

L314Q mutation was responsible for the EOB phenotype in the *Map3k1^{L314Q/+}* mice.

Effect of the L314Q mutation on eyelid epithelial cell migration, differentiation, proliferation and cell death

We investigated whether the L314Q mutation in *Map3k1* contributed to the failure of eyelid closure by affecting eyelid epithelial cell migration, differentiation, proliferation or cell death.

Actin reorganization is a critical cellular event re-

quired for cell migration, and a reduction in the cytoplasmic accumulation of F-actin has been observed with the EOB phenotype in some gene-knockout studies [27, 32, 34]. Therefore, we examined the formation of actin filaments in the eyelid tissues of E15.5 foetuses with phalloidin. Prominent F-actin accumulation in the leading edge cells was observed in the wild-type mice, but this was not observed in the leading edge cells from the mutants (Figs. 4A and B). These data demonstrate that the L314Q mutation in *Map3k1* affects actin stress fiber formation in epithelial cells of the developing eyelid,
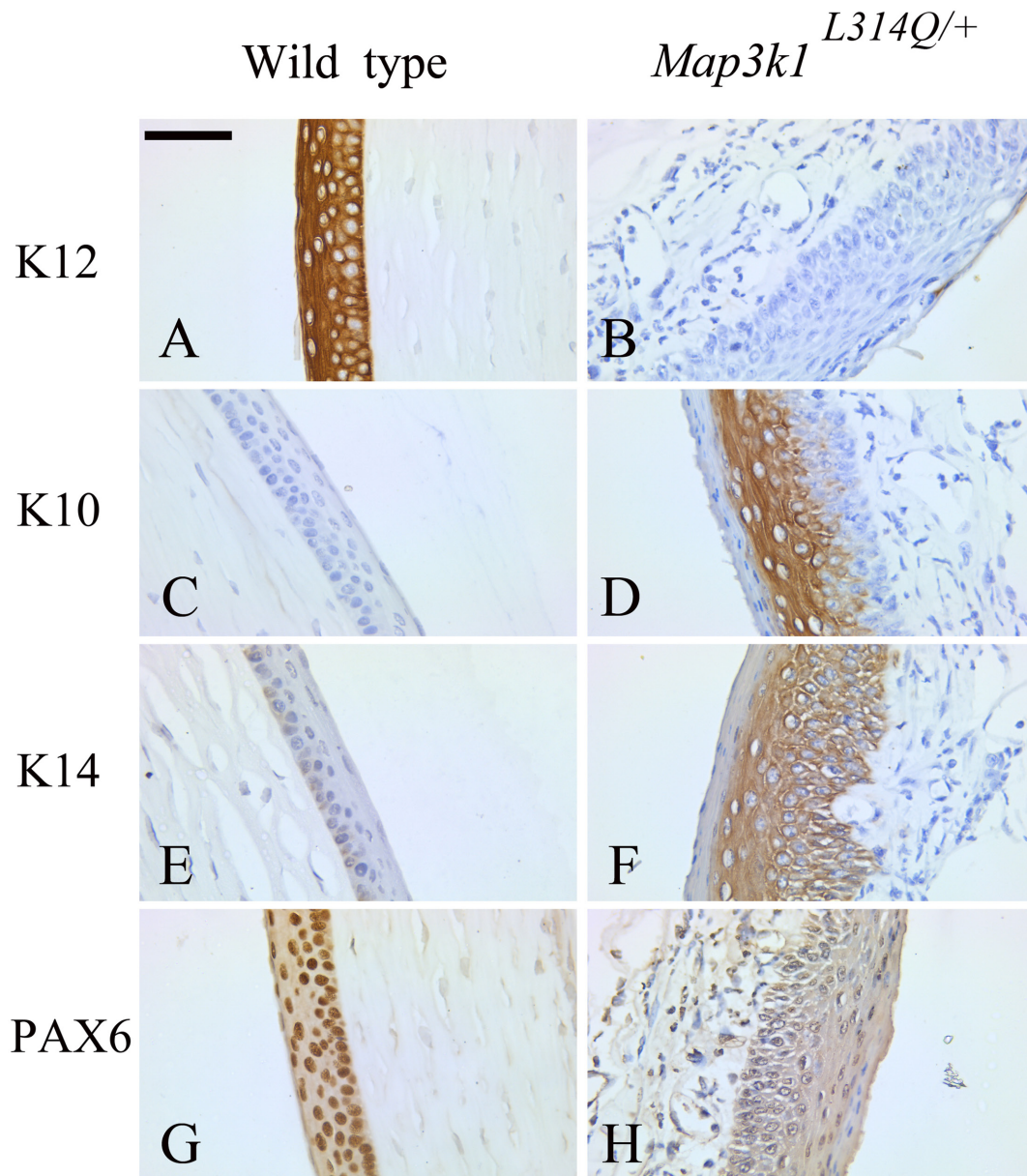
Fig. 2. Abnormal corneal epithelium differentiation in *Map3k1*^{L314Q/+} mice. (A, B) Immunostaining for keratin 12 (K12) in sections from wild-type (A) and *Map3k1*^{L314Q/+} mice (B). K12 was present in the corneal epithelium in the control corneas, but it was absent in the mutant corneas. (C, D) Immunostaining for keratin 10 (K10) in sections from wild-type (C) and *Map3k1*^{L314Q/+} mice (D). K10 was absent in the corneal epithelium in the control corneas, but it was expressed most prominently in the suprabasal epithelial layers in the mutant corneas. (E, F) Immunostaining for keratin 14 (K14) in sections from wild-type (E) and *Map3k1*^{L314Q/+} mice (F). K14 was expressed most prominently in the basal and suprabasal layers of the corneal epithelium in the mutant corneas, but it was only weakly expressed in the wild-type corneas. (G, H) Immunostaining for PAX6 in sections from wild-type (G) and *Map3k1*^{L314Q/+} mice (H). Nuclear staining of PAX6 was observed in the control corneas, but its expression was almost abolished in the mutant corneas. At least three mice were used for each analysis, and the representative data are shown. Scale bar=50 μm

which is probably associated with the failure of eyelid closure.

Eyelid epithelial cell differentiation is required for embryonic eyelid closure [3]. Periderm cells participating in temporary epithelial fusions, such as eyelid closure, express keratin 6. We, therefore, examined the levels of keratin 6 (K6). At E15.5, K6 expression was found to be similar in the periderm of both wild-type and mutant samples (Figs. 5A and B). We also performed staining for the epithelial cell differentiation marker K14 and the specific epidermal differentiation marker K10. K14 and K10 expression was also similar between the wild-type and mutant cells (Figs. 5C–F). These findings imply that the defect in eyelid closure was not caused
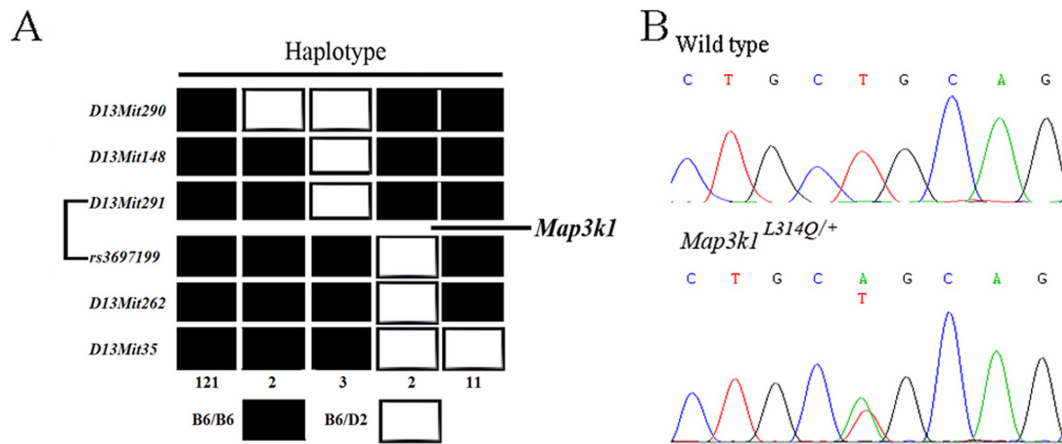
Fig. 3. Mutation mapping and identification. (A) Haplotype analysis of 139 N2 EOB mutants. Genetic markers are listed on the left side of the panel. The black boxes represent the homozygotes of B6 and the white boxes represent the heterozygotes of B6 and D2. The numbers of progeny that inherited each haplotype are shown at the bottom. The mutated gene was mapped to a region between markers *D13Mit291* and *rs3697199*. (B) Sequence analysis of the *Map3k1* gene showed a T-to-A transition mutation.
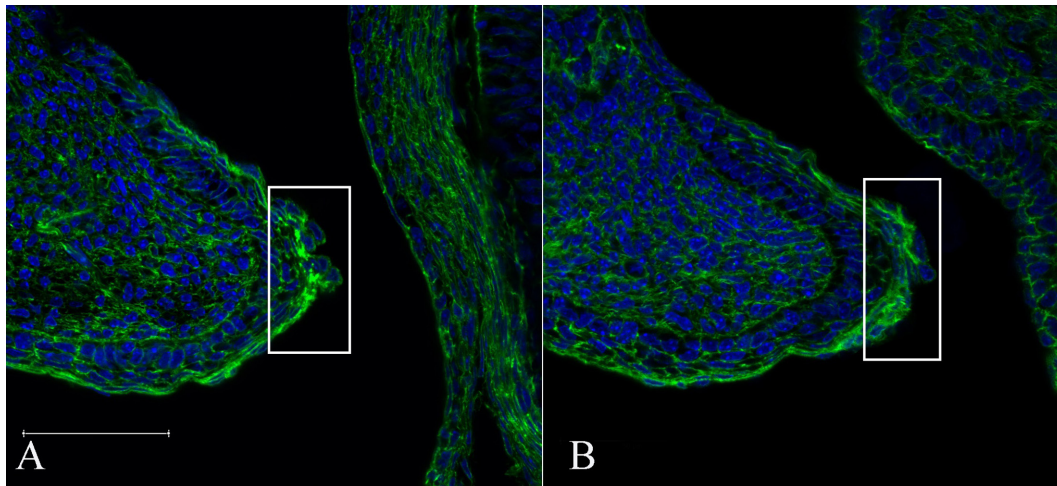
Fig. 4. Defective accumulation of F-actin in *Map3k1*$^{L314Q/+}$ eyelid epithelial leading edge cells. Staining of the eye sections from wild-type (A) and *Map3k1*$^{L314Q/+}$ (B) foetuses at E15.5 was performed using phalloidin. In the *Map-3k1*$^{L314Q/+}$ foetuses, less filamentous accumulation of F-actin was observed at the margin of the eyelid epithelium. At least three mice were used for each analysis, and the representative data are shown. Scale bar=100 μm.

by abnormalities in eyelid epithelial cell differentiation.

To further analyse other possible mechanisms responsible for EOB, wild-type and *Map3k1*$^{L314Q/+}$ embryos at E15.5 were subjected to cleaved caspase 3 labelling to examine the extent of cell apoptosis around the eyelid tissues. However, neither the wild-type nor the mutant embryos showed any apoptotic cells (Supplementary Fig. 1). Furthermore, we examined the proportion of BrdU-positive cells based on the incorporation of BrdU, which is a marker of cell proliferation, but no significant difference was observed in the eyelid epithelium between the wild-type and *Map3k1*$^{L314Q/+}$ mice (data not shown). These results demonstrate that abnormalities in cell proliferation and apoptosis did not account for the failure of eyelid closure in the *Map3k1*$^{L314Q/+}$ embryos.

Reduced level of p-JNK and c -Jun in the mutant epithelial leading edge cells

Various genetic and molecular analyses have shown that eyelid closure is dependent, at least partially, on signals transmitted through the MAP3K1-JNK axis. One of the well-defined nuclear effects of JNK is the phosphorylation of the c-Jun transcription factor and potentiation of its transcriptional activity [26, 29, 30]. Therefore, to search for the downstream effectors of the L314Q mutation in *Map3k1* during mouse embryonic eyelid development, we examined the E15.5 wild-type and *Map3k1*$^{L314Q/+}$ embryos for p-c-Jun, total c-Jun and p-JNK levels. Interestingly enough, not only p-c-Jun and p-JNK, but also c-Jun levels were decreased in the *Map-3k1*$^{L314Q/+}$ embryos (Figs. 6A–F).
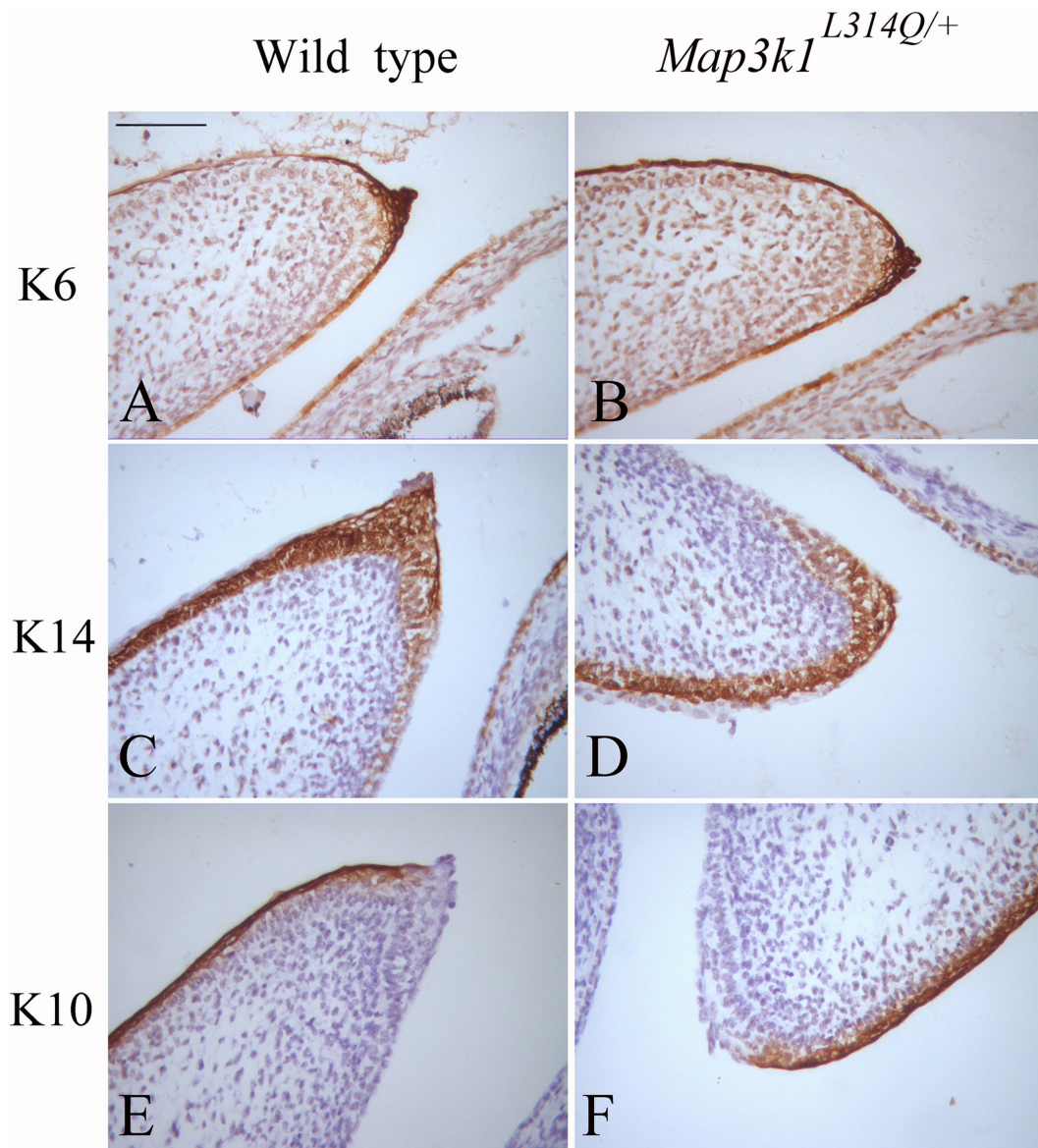
Fig. 5. Eyelid epithelial cell differentiation in *Map3k1^{L314Q/+}* mice. (A, B) Immunostaining for keratin 6 (K6) in sections from wild-type (A) and *Map3k1^{L314Q/+}* mice (B). (C, D) Immunostaining for keratin 14 (K14) in sections from wild-type (C) and *Map3k1^{L314Q/+}* mice (D). (E, F) Immunostaining for keratin 10 (K10) in sections from wild-type (E) and *Map3k1^{L314Q/+}* mice (F). At least three mice were used for each analysis, and the representative data are shown. Scale bar=100 μm.

Discussion

In the present study, we established mutant *Map3k1^{L314Q}* mice with the EOB phenotype and identified the mutation responsible for the eyelid closure defect.

We found that the eyelid closure defect in *Map3k1^{L314Q}* mice was associated with a corneal opacity phenotype. K12 is specifically expressed in the corneal epithelium in a differentiation-dependent manner. Similar to other keratins, K12 is required for the formation of cytoskeletal intermediate filaments and, thus, the maintenance of corneal epithelial integrity. In the present study, immunohistochemistry findings showed that corneal-specific K12 is replaced by skin-specific K10; this indicates the pathological conversion of CECs into skin-like epithelial cells. This explains the histological basis of the corneal opacity phenotype in the mice. Further, we found that PAX6 expression was almost abolished in the cornea of *Map3k1^{L314Q}* mice. PAX6 plays a central role in corneal epithelial cell fate determination. These findings indicate that abnormal eyelid epithelial cell differentiation may be associated with the corneal opacity phenotype. Thus, the mouse model established in this study might be useful for studying the pathomechanisms of corneal disorders.

MAP3K1 is one of the best-studied MAP3Ks. It is a
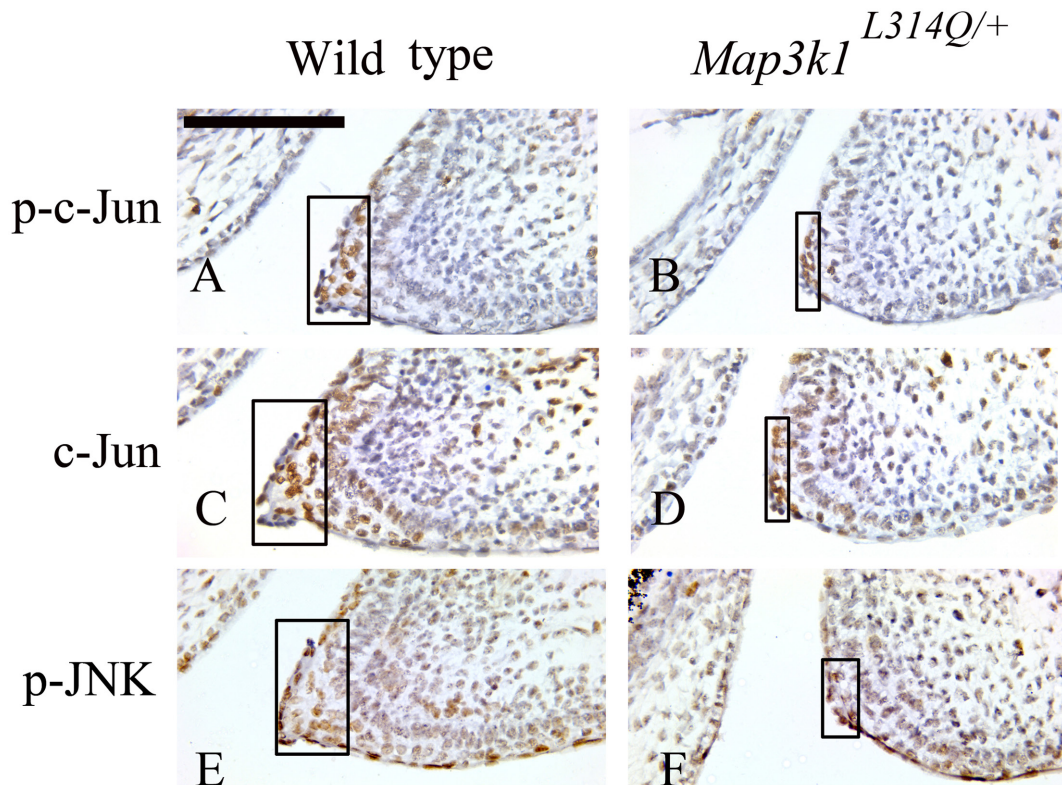
Fig. 6. Decreased levels of p-c-Jun, c-Jun and p-JNK in the eyelid epithelium of *Map3k1^{L314Q/+}* mice. (A, B) Immunostaining for p-c-Jun in sections from wild-type (A) and *Map3k1^{L314Q/+}* mice (B). (C, D) Immunostaining for c-Jun in sections from wild-type (C) and *Map3k1^{L314Q/+}* mice (D). (E, F) Immunostaining for p-JNK in sections from wild-type (E) and *Map3k1^{L314Q/+}* mice (F). At least three mice were used for each analysis, and the representative data are shown. Scale bar=100 *µ*m.

196-kDa protein with a large N-terminal regulatory domain and a C-terminal kinase domain. In mice, homozygous deletion of either the entire polypeptide (*Map3k1*-null or *Map3k1^{−/−}*) or the kinase domain (*Map3k1^{ΔKD/ΔKD}*) of MAP3K1 results in the EOB phenotype. The heterozygous mutants, however, have normal eyelid closure, underscoring the recessive nature of the mutant alleles [30, 32, 35]. However, heterozygous mutants of *Map3k1^{L314Q}* mice are born with an EOB phenotype on a B6 background; this is suggestive of a dominant mode of inheritance. Whether the difference in the mode of inheritance between *Map3k1^{−}* and *Map3k1^{L314Q}* mice was due to allelic variance or their genetic background is uncertain, because the *Map3k1^{−}* mice were maintained on a mixed genetic background of C57BL/6J and 129. Therefore, *Map3k1^{L314Q/+}* mice with the B6 background were mated with 129 mice to generate (B6 × 129) F1 mice. None of the (B6 × 129) F1 offspring exhibited the EOB phenotype; thus, the difference between the *Map3k1^{−}* and *Map3k1^{L314Q}* mice may be attributed to differences in the genetic background of the mice. This indicates that the EOB phenotype may be affected by one or more modifier genes. The *Map3k1^{ΔKD/+}* mice were backcrossed onto the C57BL6/J background for 10 gen-

erations, resulting in >99.9% B6 genomes in the knock-out line [36]. This implies that the variation between *Map3k1^{ΔKD}* and *Map3k1^{L314Q}* mice is caused by the type of *Map3k1* mutation. Immunohistochemical analyses show that *Map3k1^{ΔKD/ΔKD}* foetuses exhibit decreased phosphorylation of MAP2K4 and JNK in the eyelid tip epithelial cells. In this study, too, immunohistochemical analyses showed that the *Map3k1^{L314Q/+}* foetuses exhibit decreased phosphorylation of JNK in the eyelid epithelial cells. Genetic analyses have shown that although one functional *Map3k1* allele is sufficient for normal eyelid closure in *Map3k1^{ΔKD/+}* mice, it becomes haploinsufficient for eyelid closure in *Map3k1^{L314Q/+}* mice. This difference implies that other key regulators of eyelid closure may be inhibited in *Map3k1^{L314Q/+}* mice. The present findings show that total c-Jun in the eyelid epithelial cells were indeed reduced in *Map3k1^{L314Q/+}* embryos.

In conclusion, this study identifies a novel mouse *Map3k1* allele causing EOB phenotype and the EOB phenotype in *Map3k1^{L314Q}* mouse may be associated with the reduced level of p-JNK and c-Jun, which was supported by genetic and immunohistochemical analyses.

References

1. Findlater GS, McDougall RD, Kaufman MH. Eyelid development, fusion and subsequent reopening in the mouse. J Anat. 1993; 183: 121–129. [Medline]
2. Harris MJ, McLeod MJ. Eyelid growth and fusion in fetal mice. A scanning electron microscope study. Anat Embryol (Berl). 1982; 164: 207–220. [Medline] [CrossRef]
3. Huang J, Dattilo LK, Rajagopal R, Liu Y, Kaartinen V, Mishina Y, et al. FGF-regulated BMP signaling is required for eyelid closure and to specify conjunctival epithelial cell fate. Development. 2009; 136: 1741–1750. [Medline] [CrossRef]
4. Meng Q, Mongan M, Carreira V, Kurita H, Liu CY, Kao WW, et al. Eyelid closure in embryogenesis is required for ocular adnexa development. Invest Ophthalmol Vis Sci. 2014; 55: 7652–7661. [Medline] [CrossRef]
5. Xia Y, Kao WW. The signaling pathways in tissue morphogenesis: a lesson from mice with eye-open at birth phenotype. Biochem Pharmacol. 2004; 68: 997–1001. [Medline] [CrossRef]
6. Yu Z, Bhandari A, Mannik J, Pham T, Xu X, Andersen B. Grainyhead-like factor Get1/Grhl3 regulates formation of the epidermal leading edge during eyelid closure. Dev Biol. 2008; 319: 56–67. [Medline] [CrossRef]
7. Byun TH, Kim JT, Park HW, Kim WK. Timetable for upper eyelid development in staged human embryos and fetuses. Anat Rec (Hoboken). 2011; 294: 789–796. [Medline] [CrossRef]
8. Geh E, Meng Q, Mongan M, Wang J, Takatori A, Zheng Y, et al. Mitogen-activated protein kinase kinase kinase 1 (MAP3K1) integrates developmental signals for eyelid closure. Proc Natl Acad Sci USA. 2011; 108: 17349–17354. [Medline] [CrossRef]
9. Zieske JD. Corneal development associated with eyelid opening. Int J Dev Biol. 2004; 48: 903–911. [Medline] [CrossRef]
10. Chen B, Chen L, Zhou Y, Mi T, Chen DY, Chen L, et al. Multiple abnormalities due to a nonsense mutation in the Alx4 gene. Genet Mol Res. 2013; 12: 2771–2778. [Medline] [CrossRef]
11. Curtain M, Heffner CS, Maddox DM, Gudis P, Donahue LR, Murray SA. A novel allele of Alx4 results in reduced Fgf10 expression and failure of eyelid fusion in mice. Mamm Genome. 2015; 26: 173–180. [Medline] [CrossRef]
12. Gage PJ, Qian M, Wu D, Rosenberg KI. The canonical Wnt signaling antagonist DKK2 is an essential effector of PITX2 function during normal eye development. Dev Biol. 2008; 317: 310–324. [Medline] [CrossRef]
13. Hassemer EL, Le Gall SM, Liegel R, McNally M, Chang B, Zeiss CJ, et al. The waved with open eyelids (woe) locus is a hypomorphic mouse mutation in Adam17. Genetics. 2010; 185: 245–255. [Medline] [CrossRef]
14. Juriloff DM, Harris MJ, Mah DG. The open-eyelid mutation, lidgap-Gates, is an eight-exon deletion in the mouse Map3k1

15. gene. Genomics. 2005; 85: 139–142. [Medline] [CrossRef]
15. Kato S, Mohri Y, Matsuo T, Ogawa E, Umezawa A, Okuyama R, et al. Eye-open at birth phenotype with reduced keratinocyte motility in LGR4 null mice. FEBS Lett. 2007; 581: 4685–4690. [Medline] [CrossRef]
16. Kuracha MR, Siefker E, Licht JD, Govindarajan V. Spry1 and Spry2 are necessary for eyelid closure. Dev Biol. 2013; 383: 227–238. [Medline] [CrossRef]
17. Li C, Guo H, Xu X, Weinberg W, Deng CX. Fibroblast growth factor receptor 2 (Fgfr2) plays an important role in eyelid and skin formation and patterning. Dev Dyn. 2001; 222: 471–483. [Medline] [CrossRef]
18. Li G, Gustafson-Brown C, Hanks SK, Nason K, Arbeit JM, Pogliano K, et al. c-Jun is essential for organization of the epidermal leading edge. Dev Cell. 2003; 4: 865–877. [Medline] [CrossRef]
19. Luetteke NC, Phillips HK, Qiu TH, Copeland NG, Earp HS, Jenkins NA, et al. The mouse waved-2 phenotype results from a point mutation in the EGF receptor tyrosine kinase. Genes Dev. 1994; 8: 399–413. [Medline] [CrossRef]
20. Luetteke NC, Qiu TH, Peiffer RL, Oliver P, Smithies O, Lee DC. TGF alpha deficiency results in hair follicle and eye abnormalities in targeted and waved-1 mice. Cell. 1993; 73: 263–278. [Medline] [CrossRef]
21. Mann GB, Fowler KJ, Gabriel A, Nice EC, Williams RL, Dunn AR. Mice with a null mutation of the TGF alpha gene have abnormal skin architecture, wavy hair, and curly whiskers and often develop corneal inflammation. Cell. 1993; 73: 249–261. [Medline] [CrossRef]
22. Miettinen PJ, Berger JE, Meneses J, Phung Y, Pedersen RA, Werb Z, et al. Epithelial immaturity and multiorgan failure in mice lacking epidermal growth factor receptor. Nature. 1995; 376: 337–341. [Medline] [CrossRef]
23. Mine N, Iwamoto R, Mekada E. HB-EGF promotes epithelial cell migration in eyelid development. Development. 2005; 132: 4317–4326. [Medline] [CrossRef]
24. Parker A, Cross SH, Jackson IJ, Hardisty-Hughes R, Morse S, Nicholson G, et al. The goya mouse mutant reveals distinct newly identified roles for MAP3K1 in the development and survival of cochlear sensory hair cells. Dis Model Mech. 2015; 8: 1555–1568. [Medline]
25. Smith RS, Zabaleta A, Kume T, Savinova OV, Kidson SH, Martin JE, et al. Haploinsufficiency of the transcription factors FOXC1 and FOXC2 results in aberrant ocular development. Hum Mol Genet. 2000; 9: 1021–1032. [Medline] [CrossRef]
26. Takatori A, Geh E, Chen L, Zhang L, Meller J, Xia Y. Differential transmission of MEKK1 morphogenetic signals by JNK1 and JNK2. Development. 2008; 135: 23–32. [Medline] [CrossRef]
27. Tao H, Shimizu M, Kusumoto R, Ono K, Noji S, Ohuchi H. A dual role of FGF10 in proliferation and coordinated migration of epithelial leading edge cells during mouse eyelid development. Development. 2005; 132: 3217–3230. [Medline] [CrossRef]
28. Vassalli A, Matzuk MM, Gardner HA, Lee KF, Jaenisch R. Activin/inhibin beta B subunit gene disruption leads to defects in eyelid development and female reproduction. Genes Dev. 1994; 8: 414–427. [Medline] [CrossRef]
29. Weston CR, Wong A, Hall JP, Goad ME, Flavell RA, Davis RJ. The c-Jun NH2-terminal kinase is essential for epidermal growth factor expression during epidermal morphogenesis. Proc Natl Acad Sci USA. 2004; 101: 14114–14119. [Medline] [CrossRef]
30. Yujiri T, Ware M, Widmann C, Oyer R, Russell D, Chan E, et al. MEK kinase 1 gene disruption alters cell migration and c-Jun NH2-terminal kinase regulation but does not cause a measurable defect in NF-kappa B activation. Proc Natl Acad Sci USA. 2000; 97: 7272–7277. [Medline] [CrossRef]
31. Zenz R, Scheuch H, Martin P, Frank C, Eferl R, Kenner L, et al. c-Jun regulates eyelid closure and skin tumor development

through EGFR signaling. Dev Cell. 2003; 4: 879–889. [Medline] [CrossRef]

32. Zhang L, Wang W, Hayashi Y, Jester JV, Birk DE, Gao M, et al. A role for MEK kinase 1 in TGF-beta/activin-induced epithelium movement and embryonic eyelid closure. EMBO J. 2003; 22: 4443–4454. [Medline] [CrossRef]

33. Ouyang H, Xue Y, Lin Y, Zhang X, Xi L, Patel S, et al. WN-T7A and PAX6 define corneal epithelium homeostasis and pathogenesis. Nature. 2014; 511: 358–361. [Medline] [CrossRef]

34. Meng Q, Mongan M, Wang J, Tang X, Zhang J, Kao W, et al. Epithelial sheet movement requires the cooperation of c-Jun and MAP3K1. Dev Biol. 2014; 395: 29–37. [Medline] [CrossRef]

35. Jin C, Chen J, Meng Q, Carreira V, Tam NNC, Geh E, et al. Deciphering gene expression program of MAP3K1 in mouse eyelid morphogenesis. Dev Biol. 2013; 374: 96–107. [Medline] [CrossRef]

36. Mongan M, Meng Q, Wang J, Kao WWY, Puga A, Xia Y. Gene-Environment Interactions Target Mitogen-activated Protein 3 Kinase 1 (MAP3K1) Signaling in Eyelid Morphogenesis. J Biol Chem. 2015; 290: 19770–19779. [Medline] [CrossRef]